Available online at www.sciencedirect.com

SciVerse ScienceDirect

Physics Procedia 39 (2012) 661 – 668

Physics Procedia

LANE 2012

# Micro/nano-structuring of medical stainless steel using femtosecond laser pulses

C.Y. Lin[a], C.W. Cheng[a,*], K.L. Ou[b,c,d]

[a]*ITRI South, Industrial Technology Research Institute, No. 8, Gongyan Rd., Liujia Shiang, Tainan County 734, Taiwan, R.O.C.*

[b]*Research Center for Biomedical Devices, Taipei Medical University, Taipei 110, Taiwan, R.O.C.*

[c]*Research Center for Biomedical Implants and Microsurgery Devices, Taipei Medical University, Taipei 110, Taiwan, R.O.C.*

[d]*Graduate Institute of Biomedical Materials and Engineering, Taipei Medical University, Taipei 110, Taiwan, R.O.C.*

**Abstract**

The medical stainless steel (SUS 304) surface is irradiated by femtosecond laser pulses with linear or circular polarization to form nanostructure-covered conical microstructures. The mean spacing of the conical microstructures and the type of the nanostructure can be controlled by the laser-processing parameters. The liquid test (water and normal-saline solution) demonstrates that the process provides a fast single-step structuring method to generate hydrophobic-enhanced metal parts. The biocompatibility test demonstrated that the femtosecond laser micro/nano-structuring surfaces have excellent biocompatibility properties compared to an untreated surface.



*Keywords:* femtosecond laser; FLIPSS; hydrophobic

## 1. Motivation/State of the Art

Femtosecond laser machining has been demonstrated as an effective tool for surface micro/nano modification of materials due to its production of less debris contamination, reproducibility, and a resulting minimal heat-affected zone. When a metal surface is irradiated with femtosecond laser pulses, ripples or quasi-periodic nanostructures or self-organized structures can be formed in a simple one-step process [1]. The structures formed by this technique are usually referred to as femtosecond-laser-induced

* Corresponding author. Tel.: +886-6-6939017 ; fax: +886-6-6939059 .
*E-mail address*: CWCheng@itri.org.tw .

 doi:10.1016/j.phpro.2012.10.086

periodic surface structures (FLIPSS). The terms “ripples” and “self-organized” refer to the fact that the surface features are formed spontaneously under ultrafast laser irradiation, with the feature size much smaller than that of the irradiated area. FLIPSS have recently drawn great attention in the micromachining community. Ultra-low-reflectance metal surfaces have been prepared using FLIPSS [2]. The polarization-controlled FLIPSS enable novel laser color marking on stainless steel [3]. Although FLIPSS technique has been widely applied in studying stainless steel materials [1, 4–7], information regarding the biocompatibility properties of FLIPSS-treated surfaces remains scarce.

In this study, single-step micro/nano-structuring of medical stainless steel (SUS 304) using femtosecond laser technique is demonstrated. Using careful control of the FLIPSS structuring process, special lotus-leaf-like structures (micro/nano hierarchical structures) on the medical stainless steel can be generated. Properties of treated samples were evaluated using a biocompatibility test.

## 2. Experimental Procedures

A mechanically polished stainless steel (SUS 304) was structured in air using an 800 nm wavelength regenerative amplified Ti:Sapphire laser (SPITFIRE, Spectra-Physics) operated at a 1 kHz repetition rate. The pulse duration was 120 fs and the maximum available pulse energy was 3.5 mJ. The laser beam was linearly polarized and spatially filtered, resulting in an essentially Gaussian profile. A quarter-wave plate converted the polarization from linear to circular when necessary. The machining lens was a long working distance 10× objective lens with 0.26 NA (M Plan Apo NIR, Mitutoyo). The position of the objective lens could be adjusted vertically (i.e., Z-axis). Structures were produced by translating the sample by using an X–Y stage. In order to increase the throughput and reduce the diffraction effect, the laser beam was focused at positions below the surface of the SUS 304, i.e. 0.48 mm. The surface characteristics of the laser-treated SUS 304 were measured using scanning electron microscopy (SEM). To investigate the wettability of fabricated surfaces, a contact angle instrument with different test liquids, (e.g., distilled water and normal-saline solution) was used.

Biocompatibility testing of the FLIPSS-treated SUS 304 samples was performed according to the ISO 10993-5. The FLIPSS-treated specimens and control (untreated SUS 304) were cell (NIH3T3) cultured, and then the morphology and proliferation of the cells were observed. The specimens were placed into a 24-well polystyrene plate. The NIH3T3 fibroblasts cell suspension with a density of $1\times10^4$ cell/cm$^2$ was added into the plate. The specimens were cultured for various periods of time, i.e. 8 h, 24 h and 72 h. Following cell culture, the cells that had not attached were washed away using phosphate-buffered saline. Into every culture plate, 3-[4,5-dimethylthiazol-2-yl]-2,5-diphenyltetrazolium bromide (MTT) label solution was added. The extent of adhesion and proliferation of NIH3T3 cells on the FLIPSS-treated SUS 304 was evaluated through the observations of cell morphologies by using SEM, calculating the cell count with hemocytometer and performing an MTT assay to obtain the cell optical density (OD) by the plate reader (ELISA, DYNEX-MRX II) at $\lambda$= 595 nm.

## 3. Results and Discussion

Fig. 1 shows photographs of patterns fabricated on the SUS 304 surface using different FLIPSS processing parameters (see Table 1). The effects of the laser fluence, scanning speed and polarization type (i.e. linear or circular) were investigated. The laser fluences were set to 6.8 J/cm$^2$, which is significantly larger than the ablation threshold fluence for the stainless steel material [8].

Table 1. Laser parameters used for the FLIPSS experiments

| Sample number | Laser fluence (J/cm$^2$) | Scanning speed (mm/s) | Polarization type |
|---|---|---|---|
| A1 | 6.8 | 2 | Linear |
| A2 | 6.8 | 0.85 | Linear |
| A3 | 6.8 | 2 | Circular |
| A4 | 6.8 | 0.85 | Circular |

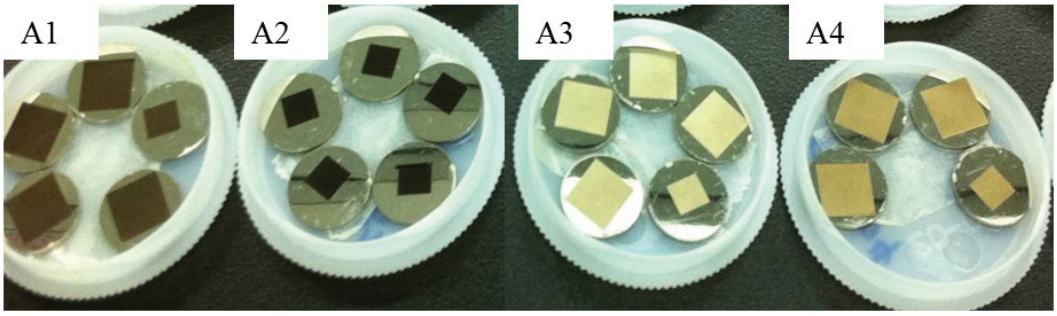


Fig. 1. Photograph of the samples after femtosecond laser irradiation

In order to study the wettability of the fabricated patterns, the analyzed areas were made by scanning to exceed 8× 8 mm$^2$ in size. In Fig. 1, it can be seen that most of the laser-irradiated surfaces, the textured regions, appear opaque.

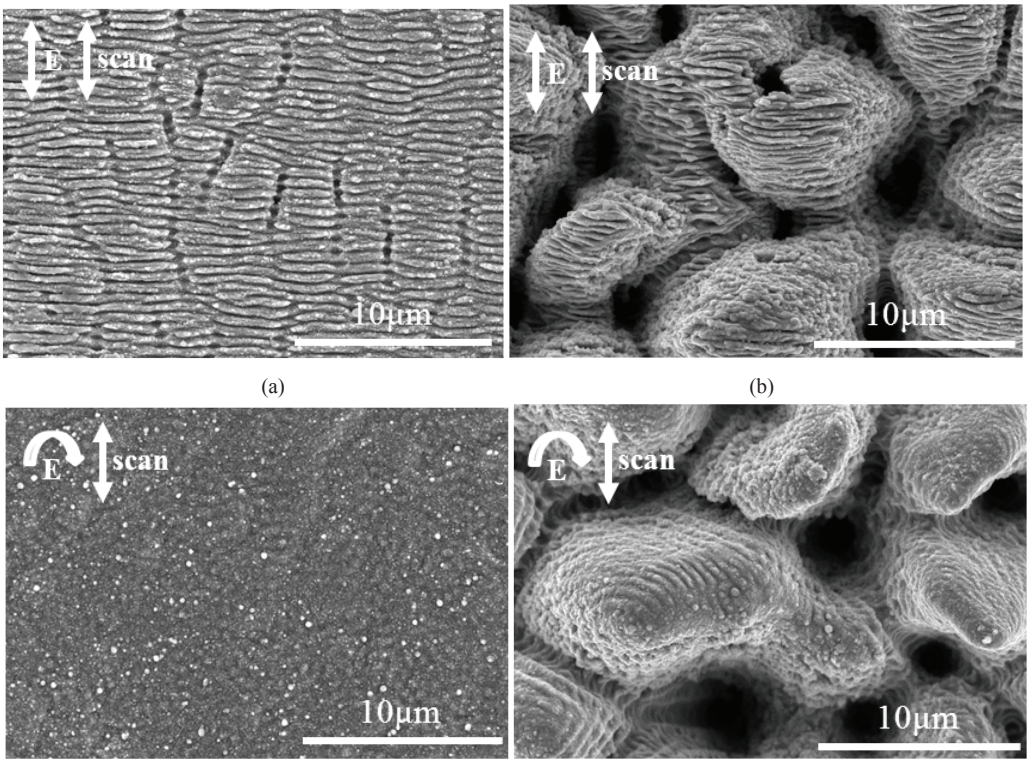


Fig. 2. FE-SEM images of the fabricated samples: (a) A1; (b)A2; (c)A3; (d)A4

Fig. 2 presents SEM images of the fabricated samples A1-A4. As seen from Fig. 2(a), the periodic-like nanostructures with periods of 600~700 nm were formed, this being slightly less than the laser wavelength at 800 nm in free space. The orientation was approximately perpendicular to the direction of the polarization (E) of the laser beam. The result agrees with previous studies that used a linearly polarized femtosecond laser beam [9]. As seen from Fig. 2(c), disordered nanostructures with feature size less than 1 μm were formed by using laser pulses with circular polarization.

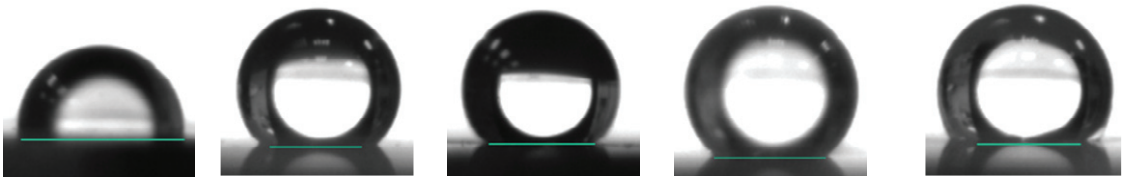


Fig. 3 Water droplet images (a) Control (contact angle: 78°); (b) A1 (contact angle: 131°); (c) A2 (contact angle: 125°); (d) A3 (contact angle: 133°); (e) A4 (contact angle: 131°)

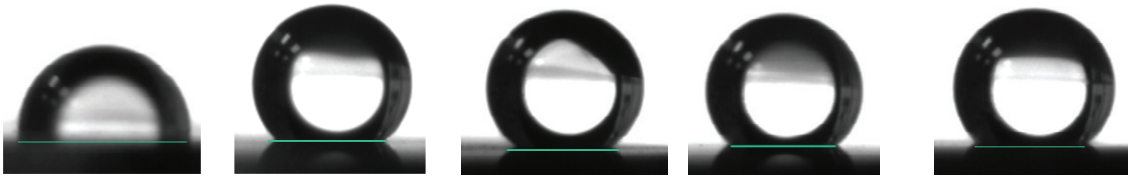

(a) (b) (c) (d) (e)

Fig. 4 Normal-saline solution droplet images (a) Control (contact angle: 86°); (b) A1 (contact angle: 133°); (c) A2 (contact angle: 138°); (d) A3 (contact angle: 134°); (e) A4 (contact angle: 136°)

As seen in Fig. 2(b) and (d), a two-scale morphology consisting of micro and nanostructures was fabricated. In Fig. 2(b), the nanostructures (similar to those observed in Fig. 2(a)) are on top of the microstructure. Similarly, in Fig. 2(d), disordered nanostructures were also superimposed with microstructures. The phenomenon is caused by the traverse of the Gaussian intensity distributed laser beam spot [5, 10]. The nanostructures are formed right after the formation of the microstructures but not simultaneously. Since the central part of the intensity of a Gaussian beam is higher than the edges, the peak power intensity can be much higher than the ablation threshold; self-organized microstructures are formed after irradiation. When the laser focus spot moves forward, the outer area with lower intensity irradiates on the microstructures, and nanostructures are formed on top of them.

Figs. 3 and 4 show images of water and normal-saline solution droplets on the SUS 304 surface, respectively. As shown in Fig. 3, the contact angles were 78° for control (non-) surface and 131°, 125°, 133° and 131° for the textured surface A1, A2, A3 and A4, respectively. This corresponds to an improvement of about 47°~55° in the water contact angle. As shown in Fig. 4, the contact angles were 86° for the control (non-treated) surface and 133°, 138°, 134° and 136° for the treated surface A1, A2, A3 and A4, respectively. This corresponds to an improvement of about 47°~52° in the normal-saline solution contact angle. In these tested liquids, the micro/nano structures increase the contact angle from hydrophilicity to hydrophobicity. The wetting state of nanostructure-covered conical microstructures can be described by the Cassie model [5, 9]. The air between the liquid droplet and the nanostructure-covered conical microstructures leads to the surface hydrophobicity.

The SEM observations of cell morphology of control (non-treated SUS 304) and sample A1 after culturing for 72 h are shown in Figs. 5(a) and (b), respectively. The cell distribution on the treated sample A1 is better than that on the control sample. As can be observed in Fig. 5(b), the FLIPSS-treated surface is almost completely covered by the cells. With the increased number of cells and improved cell viability, most of the cells had begun to grow along into the surface structures. From the higher magnification SEM images (Figs. 5(c) and (d)), it is observed that the cells exhibit good adhesion. As can be observed in Fig. 5(d), the cultured cells were strongly attached, elongated, flat and irregularly networked, probably because the surface properties, consisting of surface micro and nanostructures, and roughness affect the cell response at the micro/nano structures' interface, and enhanced cells' ingrowth. Cell differentiation and proliferation were investigated and were found to be far clearer on sample A1 than on the control sample; this implies that the cell activity in the FLIPSS-treated sample is higher than that in the control sample.

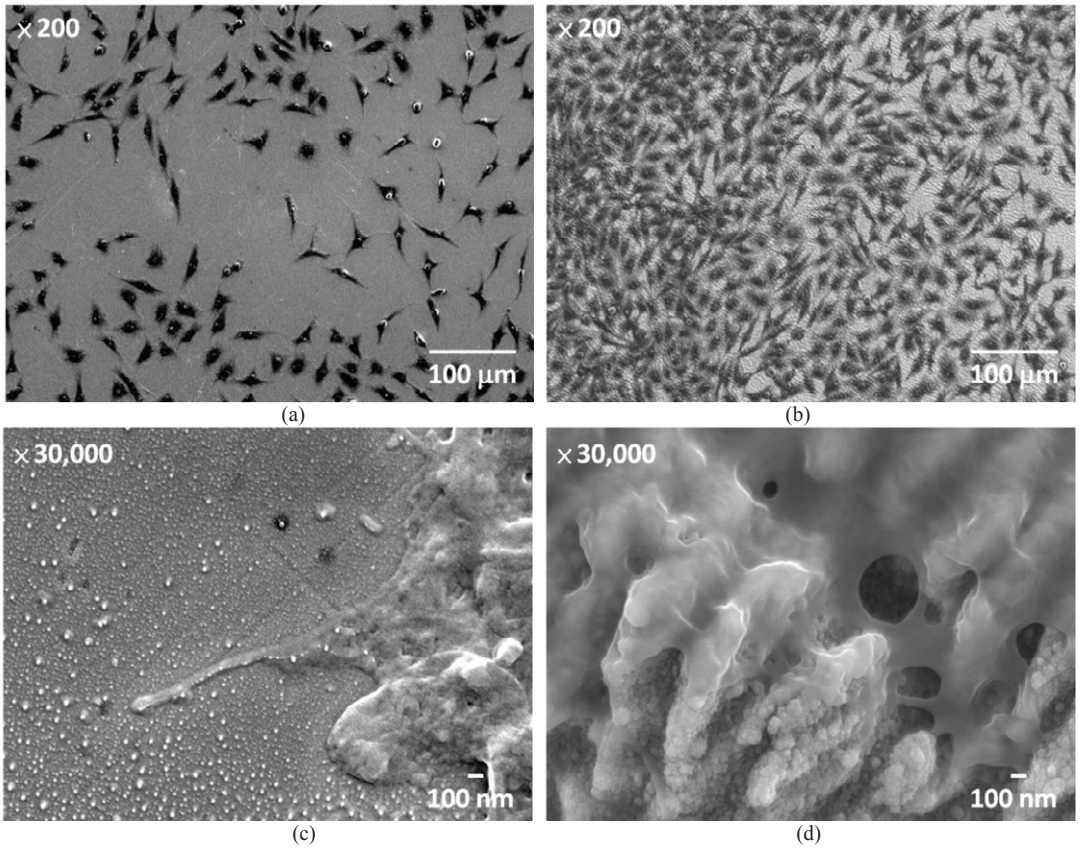


Fig. 5. FE-SEM images of an NIH3T3 cell after being in culture for 72 h: (a) control; (b) sample A1; (c) magnification of Fig. 5(a); (d) magnification of Fig. 5(b)

The results of the MTT assay with serial dilutions of the control (non-treated SUS 304) and sample A1 on NIH3T3 cells were also considered. Fig. 6 presents the cell-counting results for the control and sample A1. The cell reactions following seeding included anchorage, attachment, adhesion, migration and cell division. After 8 h in culture, the cells were attached and adhered, but not significantly spread. After 24 h of culture, the cells had spread to virtually all of the structured surfaces. More cells adhered to the sample A1 than to the control sample. The attachment assay with 72 h in culture demonstrated that significantly more cells attached to the sample A1. This means that the cells spread over the treated surface (i.e. rougher surface) more rapidly than over the non-treated surface (smooth surface). These FLIPSS-treated surface characteristics have been found to improve wettability and also to promote cell proliferation, adhesion and spreading. Hence, the FLIPSS-treated stainless steels are believed to possess better biocompatibility than stainless steels without surface modification.

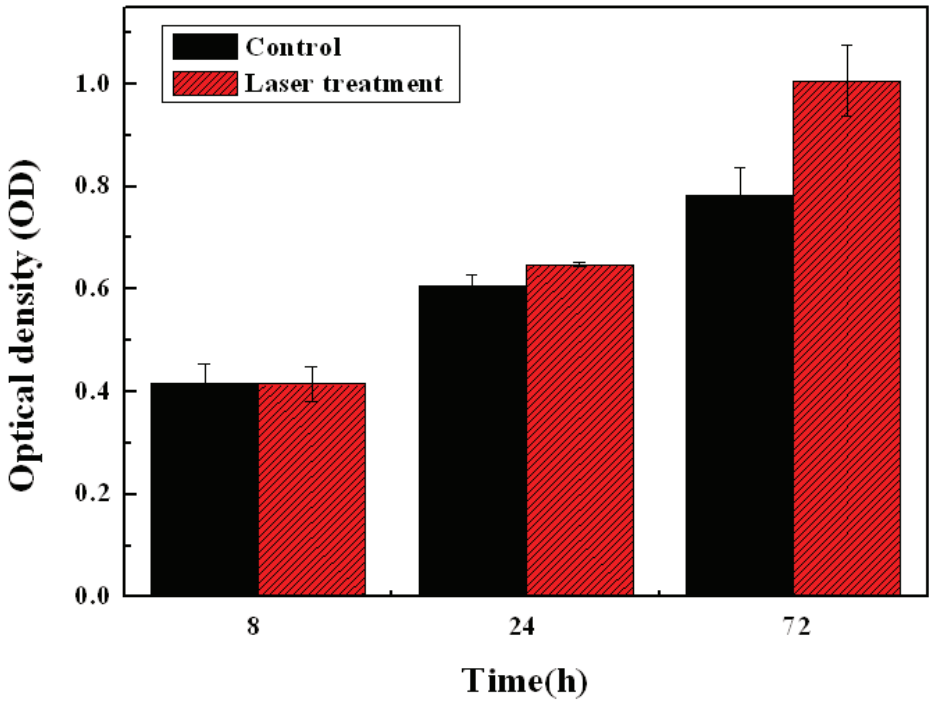


Fig. 6. MTT assay results after exposure of NIH3T3 cells on the control and A1

## 4. Results and Discussion

This paper reports a single-step fabrication process of hierarchical micro/nano structures on medical stainless steel with the femtosecond laser pulses. The hydrophobic property of the fabricated structures has been proven. Compared with the non-treated SUS 304 surface, the contact angle of the structured specimens has increased 47°~55° (water) and 47°~52° (normal-saline solution). From the biocompatibility test, the fabricated micro/nanostructure had good biocompatibility in the cell morphology and MTT. The surface texture was conducive to cell attachment, adhesion, migration and cell division. This method is expected to be widely used in the medical device industries.

## References

[1] B. K. Nayak, and M. C. Gupta, "Self-organized micro/nano structures in metal surfaces by ultrafast laser irradiation," *Optics and Lasers in Engineering,* vol. 48, no. 10, pp. 940-949, Oct, 2010.

[2] A. Y. Vorobyev, and C. Guo, "Enhanced absorptance of gold following multipulse femtosecond laser ablation," *Physical Review B,* vol. 72, no. 19, Nov, 2005.

[3] B. Dusser, Z. Sagan, H. Soder *et al.*, "Controlled nanostructrures formation by ultra fast laser pulses for color marking," *Optics Express,* vol. 18, no. 3, pp. 2913-2924, Feb 1, 2010.

[4] A. M. Kietzig, S. G. Hatzikiriakos, and P. Englezos, "Patterned Superhydrophobic Metallic Surfaces," *Langmuir,* vol. 25, no. 8, pp. 4821-4827, 2009.

[5] B. Wu, M. Zhou, J. Li *et al.*, "Superhydrophobic surfaces fabricated by microstructuring of stainless steel using a femtosecond laser," *Applied Surface Science,* vol. 256, no. 1, pp. 61-66, Oct, 2009.

[6] L. T. Qi, K. Nishii, and Y. Namba, “Regular subwavelength surface structures induced by femtosecond laser pulses on stainless steel,” *Optics Letters,* vol. 34, no. 12, pp. 1846-1848, 2009.

[7] V. V. Iyengar, B. K. Nayak, and M. C. Gupta, “Ultralow reflectance metal surfaces by ultrafast laser texturing,” *Applied Optics,* vol. 49, no. 31, pp. 5983-5988, 2010.

[8] P. T. Mannion, J. Magee, E. Coyne *et al.*, “The effect of damage accumulation behaviour on ablation thresholds and damage morphology in ultrafast laser micro-machining of common metals in air,” *Applied Surface Science,* vol. 233, no. 1-4, pp. 275-287, 2004.

[9] P. Bizi-Bandoki, S. Benayoun, S. Valette *et al.*, “Modifications of roughness and wettability properties of metals induced by femtosecond laser treatment,” *Applied Surface Science,* vol. 257, no. 12, pp. 5213-5218, 2011.

[10] V. Oliveira, S. Ausset, and R. Vilar, “Surface micro/nanostructuring of titanium under stationary and non-stationary femtosecond laser irradiation,” *Applied Surface Science,* vol. 255, no. 17, pp. 7556-7560, Jun, 2009.